JBC Papers in Press. Published on April 12, 2007 as Manuscript M611548200
The latest version is at http://www.jbc.org/cgi/doi/10.1074/jbc.M611548200

THERMODYNAMIC INVESTIGATION OF THE ROLE OF CONTACT RESIDUES OF BLIP FOR BINDING TO TEM-1 β-LACTAMASE

Jihong Wang[1], Zhen Zhang[2], Timothy Palzkill[2,3,4], and Dar-Chone Chow[1, 2,*]
From the Department of Chemistry, University of Houston, Houston, TX 77204-5003
and
[2]Structural and Computational Biology and Molecular Biophysics Program, [3]Department of Biochemistry and Molecular Biology, [4]Department of Molecular Virology and Microbiology, Baylor College of Medicine, Houston, TX 77030
Running Title: Energetic combination in BLIP - TEM-1 binding
Address correspondance to: Dar-Chone Chow, Department of Chemistry, University of Houston, Houston, TX 77204-5003, Tel. 713-743-1798, Fax. 713-743-2709, Email: dchow@mail.uh.edu

We have determined the thermodynamics of binding for the interaction between TEM-1 β-lactamase and a set of alanine substituted contact residue mutants of β-lactamase inhibitory protein (BLIP) using isothermal titration calorimetry. The binding enthalpies for these interactions are highly temperature dependent, with negative binding heat capacity changes ranging from –800 to –271 cal mol^{-1} K^{-1}. The isoenthalpic temperatures (at which the binding enthalpy is zero) of these interactions range from 5 to 38 °C. The changes of isoenthalpic temperature were used as an indicator of the changes of enthalpy and entropy driving forces, which in turn are related to hydrophobic and hydrophilic interactions. A contact residue of BLIP is categorized as a canonical residue if its alanine substitution mutant exhibits a change of isoenthalpic temperature matching the change of hydrophobicity due to the mutation. A contact position exhibiting a change in isoenthalpic temperature that does not match the change in hydrophobicity is categorized as an anti-canonical residue. Our experimental results reveal that the majority of residues where alanine substitution results in a loss of affinity are canonical (seven out of ten), and about half of the residues where alanine substitutions have a minor effect are canonical. The interactions between TEM-1 β-lactamase and BLIP canonical contact residues contribute directly to binding free energy, suggesting potential anchoring sites for binding partners. The anti-canonical behavior of certain residues may be the result of mutation-induced modifications such as structural rearrangements affecting contact residue configurations. Structural inspection of BLIP suggests that the Lys^{74} side chain electrostatically holds BLIP loop 2 in position to bind to TEM-1 β-lactamase, explaining a large loss of entropy-driven binding energy of the K74A mutant and the resulting anti-canonical behavior. The anti-canonical behavior of the W150A mutant may also be due to structural rearrangements. Finally, the affinity enhancing effect of the contact residue mutant Y50A may be due to energetic coupling interactions between Asp^{49} and His^{41}.

Protein–protein interactions are critical for any living organism. Their roles are vital in most biological processes, including metabolism, immune responses, signal transduction, gene regulation, and enzymatic regulation. Most noncovalent protein-protein interactions involve many contacts and interactions, which in turn combine into a macromolecular binding interaction with the needed specificity and affinity. Understanding the principles behind the affinities and specificities of protein-protein interactions will provide leads in developing new methods and reagents for protein-protein interactions. Recent advances in the structural biology of protein-protein interactions have revealed the complexity of structure-function relationships (1).

In general, a protein-protein binding interaction involves a relatively planar interface with a large contact interface area (typically > 1000 Å^2) and a large number of contact residues (>10) (2-4). With a maximal contribution of 120 cal/(mol Å^2), the typical interaction strength of

-13 kcal/mol is only a fraction of the maximum available (5). One major consistent observation of many studies is the presence of so-called hot spots in protein-protein interactions (6-9). Among all the contact residues, only a small subset (called hot spot residues) contributes the majority of the binding free energy (9). The alanine substitution of any of these hot spot contact residues results in a significant loss of binding free energy, while the alanine substitution of other contact residues does not change the binding free energy.

Based on simple physical considerations, the sidechain of a contact residue could contribute to the binding energy of a complex either directly or indirectly, or both. Direct contributions are the result of the favorable interactions between the sidechain and the interacting protein partner. Indirect contributions result from the enhancement by the contact residue to other contact residues (energetic coupling) and/or the alteration of contact interactions due to structural rearrangements. With limited structural and binding information, predicting the direct and indirect contributions from a contact residue is difficult. In this study, the binding thermodynamics (binding enthalpy, entropy, and heat capacity change in addition to binding free energy) of alanine substitutions of contact residues was determined to assess how individual contact residue contribute to the final binding free energy. The binding thermodynamics of the mutants not only describe the changes in binding affinity, but also changes of the nature of the driving forces of binding (14). For instance, a mutation that decreases the binding free energy could do so either via changes in the enthalpy or entropy driving forces or a combination of both. For residues whose side chains contribute directly to binding through interaction with the target protein, the changes in binding thermodynamics should approximately correlate with the expected changes of the physiochemical nature of mutation (e.g. a polar to nonpolar mutation should increase entropy driving forces). We categorize the contact residues whose mutations exhibit this correlation as canonical residues. For residues that make an indirect contribution to binding, the thermodynamics may not correlate with the physiochemical nature of the mutation. For example, an alanine substitution that decreases residue hydrophicity but exhibits changes in the enthalpy rather than entropy driving forces may be due to a change in the positioning of a neighboring polar residue do to the mutation of the residue under study. These contact residues are categorized as anti-canonical. The scenario of the structural rearrangement can be established with detailed structural information. The analysis of thermodynamic and structural information could provide detailed information of the role of interface residues for binding interactions and this information could be used in the future design of tight binding peptides or small molecules that could serve as inhibitors of β-lactamase.

β-Lactam based antibiotics specifically inactivate glycopeptide transpeptidases to prevent formation of bacterial cell walls thereby leading to the lysis of the bacteria. This group of antibiotics is currently among the most widely used antimicrobial therapeutics. β-lactamases provide for resistance to these antibiotics by selectively cleaving the amide bond in the β-lactam ring. There are four major classes of β-lactamases (A-D) (16). The class A β-lactamases are prevalent in the clinical setting and confer infectious bacteria with resistance to β-lactam based antibiotics. Among the class A β-lactamases, TEM-1 β-lactamase is the most prevalent among gram negative bacteria and has been a subject of concern because of its ability to hydrolyze a range of β-lactam based antibiotics (17).

BLIP is a 165 amino acid protein produced by the soil bacterium *Streptomyces clavuligerus* that potently inhibits the TEM-1 β-lactamase (18). BLIP has a tandem repeat structure of a 76 amino acid αβ domain (19). These two tandem domains form a β saddle with a relatively hydrophobic concave surface. BLIP's saddle concave surface binds on the loop-helix region of TEM-1 and extends two loops around the edge of the loop-helix section into the substrate binding pocket of the TEM-1. The Asp^{49} residue of BLIP on one of the loops (loop 1) occupies the catalytic site of TEM-1 β-lactamase (19).

The BLIP system is a protein-protein interaction model for which a relatively complete set of data of alanine-scanning experiments exist (20). The alanine-scanning analysis revealed (1) there are two hotspots on the interacting surface of BLIP, and (2) one mutation (Y50A) actually

increases binding affinity for TEM-1 β-lactamase by 50 fold (8). Several weak binding peptide inhibitors for TEM-1 have been generated, among which two are the TEM-1-contacting fragments of BLIP (21,22). The contacts of these peptides can be potentially strengthened to create tight binding inhibitors with appropriate enhancement of binding forces.

This study provides a detailed thermodynamic characterization of the interactions between TEM-1 β-lactamase and the BLIP alanine scaning mutants. The measurements and analysis have categorized the BLIP contact residues into four types: canonical hotspot, canonical nonhotspot, anti-canonical hotspot, or anti-canonical nonhotspot residues. The information generated here provides insight into the determinants of molecular recognition between BLIP and β-lactamase that should be useful in to design of BLIP derivatives with altered binding specificity.

EXPERIMENTAL PROCEDURES

Materials-Talon resin was purchased from Clontech (Mountain View, CA). Ion exchange media and columns (MonoQ 5/50 GL, HighTrap Q, Q Sepharose Fast Flow) and sizing columns (Superdex 75 10/300, Superdex 75 prep grade) were purchased from Amersham Pharmacia (Piscataway, NJ). All other reagents are reagent grade from Sigma.

Protein expression and purification — All expression DNA clones were constructed previously (8) and the proteins were expressed and purified with previously described procedure with minor modifications. Briefly, *E. coli* bacteria (strain RB791) containing BLIP mutant expression plasmid were grown in LB media containing 17.5 ug/ml chloramphenicol at 37 °C from a single clone and induced with 2 mM Lactose and 1% glycerol instead of IPTG when the OD at 600 nm was approximately 1.2. The culture was kept shaking at room temperature for 6 hours and harvested by centrifugation at 5000 rpm for 10 minutes at 6 °C. The bacterial pellets were resuspended in B-PER Bacterial Protein Extraction solution (Pierce, Rockford, IL) or a prepared equivalent (1% Trinton-X 100 in 10 mM Tris-HCl, pH 8.0, 150 mM NaCl) at a ratio of 15 ml for 1 g of bacterial pellet. The resuspensions were vigorously shaken for 20 min at room temperature, and then centrifuged at high speed (15000 rpm in a Beckman type 35 rotor) for 30 min. The supernatants were mixed by stirring with Talon cobalt resin overnight. The Talon cobalt resin was allowed to settle by gravity and then collected and washed three times. The bound BLIP mutant proteins were eluted from the Talon cobalt resins using 150 mM imidazole in TBS. The bacteria containing TEM-1 β-lactamase expression plasmid DNA was grown at 37 °C and induced at OD_{600nm} ~0.6 with 0.3 mM IPTG for 3 hours at 37 °C. The expressed periplasmic protein TEM-1 was extracted by osmotic shock in which bacteria were soaked with 20% sucrose solution at room temperature, centrifuged, and the resulting pellet was resuspended in 5 mM ice cold magnesium sulfate. The osmotic shock fluid was fractionated on a DEAE column in 10 mM Tris-HCl buffer at pH 7 with 100 mM NaCl. Flow through material was diluted 10 fold with distilled water and fractionated on the DEAE column again. TEM-1 β-lactamase was eluted with a 0-2 M NaCl gradient in Tris-HCl buffer at pH 7.0. The protein was further purified using a Superdex-75 sizing column in 50 mM phosphate buffer at pH 7.0 with 150 mM NaCl. The purity of the proteins was confirmed by SDS-PAGE analysis. Protein concentrations were determined using optical density measurements at 280 nm with 8 M guanidine HCl denatured protein, based on the theoretically calculated extinction coefficients according to the amino acid sequence.

Isothermal titration calorimetric measurement — The binding enthalpy measurements were carried out using a VP-ITC isothermal titration calorimeter from MicroCal LLC (Northampton, MA). The data processing was performed using the manufacturer-supplied software package, Origin 7.0 (OriginLab Corp., Northampton, MA) with an ITC Add-on. Typical titration experiments were carried out by titrating 40 μM TEM-1 β-lactamase into 4 μM BLIP mutant in PBS buffer (50 mM phosphate pH 7.0, 150 mM NaCl). To avoid inconsistencies from different protein preparations, we pooled enough TEM-1 β-lactamase (~60 mg) to titrate many BLIP mutants and enough wild type BLIP (~7 mg) to use as the reference for every mutant

titration. For this purpose, about 70 mg TEM-1 was made and stored in PBS buffer. The proton linkage effect was tested by measuring the binding enthalpies of some BLIP mutants and TEM-1 β-lactamase in Tris buffer. The binding enthalpy in Tris buffer was identical with that in phosphate buffer suggesting there is a minimal proton linkage effect for the determinations.

ITC experiments of each BLIP mutant binding to TEM-1 β-lactamase were done in no less than three different temperatures within the range of 6 °C to 30 °C. The typical injection volume was 15 μL with a 300 second gap between consecutive injections. Because of diffusion around the tip of the injection syringe during the lengthy waiting time before a titration starts, the first injection tends to have less signal. To minimize this effect and preserve materials, we set the first injection volume to 3 μL. During data processing, the data points from the first injections were normally removed. Binding affinities could not be determined accurately by standard ITC titration for mutants exhibiting a binding affinity to the TEM-1 β-lactamase higher than 10^8 M^{-1}, however their binding enthalpies are still valid. A displacement ITC titration was used to determine the values for high affinity binding mutants.

Displacement titrations were used to determine the binding affinities for the mutants having binding affinity to TEM-1 of 10^8 M^{-1} or more. For each tight binding mutant, we looked for a proper low affinity mutant as the competitive displaced mutant in order to adjust the overall binding constant value to between 10^5 to 10^7 M^{-1} with appropriate enthalpy signals. The tight binding affinity mutant was titrated into the pre-formed complex between TEM-1 and the lower binding affinity mutant. The resulting apparent K value and ΔH were used to calculate the K and ΔH of the tight mutant. The following equations were used to calculate the K and ΔH of the tight mutant provided the displacement ITC is competitive (25,26)

$$\Delta H_{apparent} = \Delta H_{tight} - \Delta H_{low} \frac{K_{low}[\text{mutant}_{\text{low}}]}{1 + K_{low}[\text{mutant}_{\text{low}}]} \quad \text{(Eq. 1)}$$

$$K_{apparent} = \frac{K_{tight}}{1 + K_{low}[\text{mutant}_{\text{low}}]} \quad \text{(Eq. 2)}$$

where $\Delta H_{apparent}$, ΔH_{tight}, and ΔH_{low} are the apparent enthalpy of the displacement ITC, the binding enthalpy of the tight mutant, and the binding enthalpy of the low affinity mutant, respectively. $K_{apparent}$, K_{tight}, and K_{low} are the apparent K of the displacement ITC, the K of the tight mutant, and the K of the low affinity mutant, respectively. All parameters except K_{tight} are measured either from displacement ITC or standard ITC. The first equation (Eq. 1) provides a convenient diagnostic tool to confirm that the displacement ITC is competitive. Only when the first equation (Eq. 1) is satisfied by the results of our measurements from displacement ITC and standard ITC, we are confident that the displacement ITC is competitive and the K_{tight} can be correctly estimated using the second equation (Eq. 2). We had also processed the displacement ITC data using the manufacturer-supplied subroutine that incorporated into the program package, and we find the two results are virtually identical when the displacement is competitive (less than 5% difference).

In several cases, the displacement ITC failed to show competitiveness between the high affinity mutant and the low affinity mutant for the binding of TEM-1. We did not incorporate those data in our analysis.

Structure-based estimation of thermodynamic parameters — The solvent accessible surface areas of the protein complexes of TEM-1 and BLIP mutants were calculated as follows. The structures of the complexes of TEM-1 and BLIP mutants were modeled by simple mutation on Coot (27) with the most favorable rotamer. The accessible surface areas were calculated from these modeled structures and the wild type structure (1JTG) using the program AREAIMOL from the CCP4 suite of programs with a probe of 1.4 Å (28).

Hydrophobicity calculations of the mutants — The hydrophobicity scale of the mutation was calculated according to the scale reported by Black & Mould (29). For each mutant, the hydrophobicity change was calculated by the difference between the hydrophobicity of the wild type amino acid and that of alanine.

RESULTS

Thermodynamics of binding of TEM-1 β-lactamase and wild type BLIP — Isothermal titration calorimetric measurements of the binding of TEM-1 β-lactamase to wild type BLIP (Figure 1A) were performed. At 10 °C, the binding enthalpy is highly unfavorable ($\Delta H = +5.4 \pm 0.2$ kcal mol^{-1}). The binding enthalpy is, however, strongly temperature dependent. For temperatures below 15 °C, the binding enthalpy is positive; however, at temperatures higher than 25 °C, the binding enthalpy becomes negative ($\Delta H = -3.9 \pm 0.1$ kcal mol^{-1} at 25 °C). Based on these results, we determined that the binding heat capacity change for this interaction (ΔCp) is -672 ± 35 cal$\cdot mol^{-1}\cdot K^{-1}$. Using the results for the temperature dependence of the binding enthalpy of this interaction, we extrapolated an isoenthalpic temperature (at which $\Delta H = 0$) of 19 ± 1 °C for formation of a complex between TEM-1 β-lactamase and wild type BLIP (Figure 1B). At temperatures near 19 °C (15 to 22 °C), we found that titrations are difficult to interpret because of the low signal. It was further found that standard isothermal calorimetric measurements underestimated the binding affinity of this interaction (K was determined to ~10^8 M^{-1}). The actual binding affinity is 2 x 10^9 M^{-1} (30,31); since titration conditions limited the number of data points that could be obtained in the transition region, the accuracy of the curve fitting used to obtain a binding affinity is also limited. This is a well-documented limitation in ITC titration ($K > 10^9$ M^{-1}) (32). Because of the underestimation, the binding entropy from these standard ITC measurements becomes unreliable. The enthalpy measurements obtained, however, are accurate.

To determine the binding affinity more accurately, a displacement scheme was used (33). For these experiments, a solution of known concentration of a complex of TEM-1 β-lactamase and a low affinity BLIP mutant was placed in the sample cell of the calorimeter and titrated with wild type BLIP. The injected wild type BLIP displaced the lower affinity BLIP mutant from the complex. The observed calorimetric enthalpy and K value were used to calculate the K value of the binding of wild type BLIP and TEM-1 β-lactamase based on competitive binding kinetics according to published methods (25).

Thermodynamics of binding between TEM-1 β-lactamase and BLIP mutants — We have further carried out systematic isothermal calorimetric determinations of the binding thermodynamics for the interaction of TEM-1 β-lactamase with 20 alanine substitution mutants of BLIP contact residues. Figure 2 shows representative raw titration curves of the binding interaction between a low affinity BLIP mutant and TEM-1 β-lactamase. The binding thermodynamics of 20 contact residue mutants with TEM-1 are listed in Table 1. The binding thermodynamics of hotspot residue mutants were determined by standard ITC measurements. The typical "c values" (defined as K multiplied by the concentration of protein in the sample cell) of these mutants range from 100 to 300. It has been suggested that "c values" should range from 5 to 500 for accurate determination of K values (34). Based on this criterion, the hotspot mutants are well within the appropriate range for accurate determination of binding thermodynamics (binding free energy, enthalpy and entropy). For the high affinity mutants ($K > 10^9$ M^{-1}), the c values are 2000 or higher and the K values determined by standard ITC are highly inaccurate because of the limited number of data points in the transition region of the binding curve. The standard ITC-determined K values for these high affinity mutants are at least ten fold less than that expected from the reported K_i values (20). As in case of wild type BLIP, the binding enthalpies of these high affinity mutants are accurate using standard ITC measurements.

Displacement ITC measurements — Further experiments were performed to determine the K values of a selected group of high affinity mutants using displacement ITC. To confirm that the displacement ITC method is applicable in this system, the displacement ITC measurements were performed with several combinations of high and low affinity mutants. Noteworthy results reported in Table 1 include the observation that the BLIP Y50A has higher affinity than wild type, Y51A has the most negative binding heat capacity changes, and Y143A is an anti-canonical residue (see Discussion). Some anomalies were observed in the displacement ITC experiments. For example, the titration of wild type BLIP into a mixture of the R160A mutant and TEM-1 β-

lactamase failed to exhibit any signal at temperatures below 25 °C. We hypothesize this is due to the slow off-rate of the R160A BLIP mutant. Results from noncompetitive displacement measurements were excluded from consideration.

Analysis of the binding thermodynamic parameters — At 15 °C, four hydrophobic hotspot residues, Phe^{36}, Tyr^{53}, Trp^{112} and Phe^{142} lose their entropy driving forces when replaced with alanine while the charged hotspot residues $Asp^{49}$and Arg^{160} lose their enthalpy driving forces when replaced with alanine (Figure 3). In addition, both histidine hotspot residues, His^{41} and His^{148} lose entropy driving forces at 15 °C when replaced with alanine. Unexpectedly, the charged lysine hotspot residue, Lys^{74}, loses entropy driving forces but exhibits increased enthalpy driving forces. Furthermore, the hydrophobic hotspot residue, Trp^{150}, loses enthalpy driving forces rather than entropy driving forces. The alanine substitution of three nonhotspot contact residues Tyr^{51}, Ser^{113}, Arg^{144} results in no change in either enthalpy or the entropy driving forces while substitution of four nonhotspot contact residues, Ser^{39}, Gly^{48}, Ser^{71}, and Tyr^{143} results in loss of enthalpy driving forces but the loss is compensated by increased entropy driving forces. Substitution of three other nonhotspot contact residues Tyr^{50}, Glu^{73}, Gly^{141} results in loss of entropy but this is compensated by increases in enthalpy driving forces. Finally, the enhancement of binding observed for the Y50A mutant is associated with an increase in enthalpy driving forces.

DISCUSSION

The range of the binding enthalpies determined here are within the normal range for protein-protein interactions (from –9 to +10 kcal mol^{-1} over a temperature range of 5 to 30 °C). The values of the binding heat capacity changes for these BLIP mutants and TEM-1 β-lactamase range from –271 to –800 cal mol^{-1} K^{-1} (–667 cal mol^{-1} K^{-1} for the wild type BLIP). The empirical formula: $\Delta Cp = -0.45\ \Delta ASA_{np} + 0.21\ \Delta ASA_{p}$ was used to calculate an expected binding heat capacity change of the wild type complex of –336 cal mol^{-1} K^{-1} (a value of 2636 $Å^2$ was used (19) as the total buried surface area with 55% nonpolar and 45% polar). This empirically calculated value is significantly lower than the experimentally determined value for the wild type complex. Similar observations have been made for a number of protein-protein interaction systems in which the experimental binding heat capacity changes are significantly more negative than predicted by the empirical formula (for example, human growth hormone and receptor binding has a –992 cal mol^{-1} K^{-1} experimental value and a –366 cal mol^{-1} K^{-1}empirically predicted value based on the structure) (15). It is noticeable that the empirically calculated value is closer to that of two weak mutants (W150A and D49A). Both the broad range of the experimental values and the discrepancy with the empirically predicted values show that the relationship between binding heat capacity changes and buried surface area could be influenced by other factors such as affinities. More than half of the BLIP mutants have a TEM-1 binding affinity higher than the limits of the standard VP-ITC measurements. Displacement ITC was used to determine some of those binding affinities and the values obtained match well with reported inhibition K_is (20), confirming that binding and inhibition are the same process. Despite the fact that the displacement ITC titrations have limited signal to noise, the method provided affinities with reasonable accuracy. Since free energy is a logarithmic function of the affinity constant, the resulting binding free energy appears to be well determined. Displacement ITC does, however, require more of the purified proteins and the calculated entropies do carry slightly higher error. However, even with the limitations on affinity determinations, the standard ITC does provide accurate measurements of the binding enthalpies and the binding heat capacity changes.

At least at 15 °C, the alanine substitutions of the hotspot residues cause the loss of binding free energy due either mainly from entropy or enthalpy components (see Figure 3). At the same temperature, some of the nonhotspot contact residues change their entropy driving forces when replaced with alanine, but changes in enthalpy driving forces compensate to maintain the same binding free energy. The Y50A mutant exhibits an enthalpy driving force change that increases

binding free energy by about 2 kcal/mol. One problem we encountered in using the changes of the entropy and enthalpy driving forces to characterize mutations is the characterization is temperature dependent. For instance, R160A exhibits a loss of binding free energy that is mainly due to the loss of enthalpy driving forces at 15 °C but at 6 °C the lost binding free energy is due to the losses of both enthalpy and entropy driving forces. This is because there are large differences in the binding heat capacity changes among different mutants.

To incorporate the binding heat capacity changes (ΔCp) in the characterization, the isoenthalpic temperature (T_H) was used as an indicator for hydrophobic driving forces. Based on the data, an increase of the enthalpy driving term is consistent with a decrease in isoenthalpic temperature while an increase of the entropy driving term is consistent with an increase of isoenthalpic temperature. The change in hydrophobicity of a position was calculated as the difference between the hydrophobic scale of substituted residue side chain and the wild type side chain according to Black & Mould (29). A plot of changes in hydrophobicity due to alanine substitution versus differences in isoenthalpic temperatures is shown in Figure 4. Within the relevant range of temperatures, a binding interaction that exhibits a higher isoenthalpic temperature will also exhibit a higher entropy driving term contribution. The square symbols represent the mutations that show an approximate correlation with hydrophobicity changes and isoenthalpic temperature. They reside in the lower-left and upper-right quadrants. The triangle symbols are the mutations exhibiting opposite trends in isoenthalpic temperature compared to changes of hydrophobicity. They reside in the upper-left and lower-right quadrants.

Among the BLIP contact residues, nine are polar or charged and reside in the upper half of the plot (Figure 4). The binding thermodynamics of the alanine substitution of these positions should result in increased entropy driving forces -- the isoenthalpic temperatures should increase. Eleven BLIP contact residues are nonpolar and located in the lower half of the plot, the binding thermodynamics of their alanine substitutions should show increases in enthalpy driving forces if alanine substitution is deemed to reduce hydrophobicity, or increases in entropy driving forces if alanine substitution is deemed to strengthen hydrophobic interaction. Figure 4 shows that five of the charged-polar contact residues and two of the nonpolar contact residues behave opposite to what is expected based solely on hydrophobicity. These contact residues are termed anti-canonical while those contact residues that behave as expected are termed canonical. A graphical representation of the canonical and anti-canonical contact residues on BLIP is shown in Figure 5.

Canonical contact residues — Five of the nonhotspot contact residues, Ser^{39}, Gly^{48}, Tyr^{51} Ser^{71}, and Ser^{113}, are canonical residues (Figure 4). Their alanine substitutions show relatively small changes in binding free energy, binding enthalpy or binding entropy or the isoenthalpic temperature (see Figure 3 and 4). The sidechains of these residues contribute very limited driving forces to the binding free energy or binding thermodynamics. These facts suggest the corresponding locations on TEM-1 β-lactamase are relatively inert for protein interactions.

Seven of the hotspot residues, Phe^{36}, His^{41}, Asp^{49}, Tyr^{53}, Trp^{112}, Phe^{142}, and Arg^{160} are canonical residues. The sidechains of the hydrophobic residues (Phe^{36}, Tyr^{53}, Trp^{112}, and Phe^{142}) provide relatively large entropy driving forces to the binding free energy (Figure 3 and Figure 4). Similarly, the sidechains of the charged residues (Asp^{49}, and Arg^{160}) provide relatively large enthalpy driving forces toward the binding free energy (Figure 3 and 4). These results suggest the interactions between these sidechains and TEM-1 β-lactamase directly contribute to the binding free energy. The sidechain of His^{41} provides a slightly less distinctive division between entropy and enthalpy driving forces. This may be simply due to the ambidextrous properties of the imidazole sidechain. The canonical nature of these hotspot residues suggests that the corresponding locations on the TEM-1 β-lactamase have the physiochemical properties to interact with these sidechains to provide strong binding forces. A short BLIP fragment peptide containing one of these residues (Asp^{49}) has been shown to bind and provide inhibitory activity toward TEM-1 β-lactamase (22).

Another strong canonical residue is the Tyr^{50} contact residue in that the mutant Y50A shows a large decrease in isoenthalpic temperature, suggesting an increase in hydrophilic interactions, such as hydrogen bonds and van der Waals interactions. The increase in hydrophilic interactions increases the binding free energy by more than 1.5 kcal (Figure 3). This suggests there is strong energetic coupling among the neighboring residues. The Y50 side chain collides with Val^{216}, Met^{129}, and Pro^{107} of TEM-1. The collision restricts the interactions between BLIP Asp^{49} and TEM-1 and between BLIP His^{41} and TEM-1 (see Figure 6). The increased strength of the interactions involving Asp^{49} and His^{41} after removal of the Tyr^{50} side chain is consistent with the increase in the enthalpy driving forces thereby generating the decrease in isoenthalpic temperature.

Anti-canonical residues — The Tyr^{143} contact residue is characterized as anti-canonical since the Y143A mutant shows a large increase of the isoenthalpic temperature. The Tyr^{143} side chain makes direct a contact with Glu^{104} of TEM-1 β-lactamase and an intramolecular contact with BLIP Lys^{74}. The loss of the Tyr^{143} side chain may allow better hydrophobic interactions, such as between BLIP loop 2 and TEM-1.

The negatively charged BLIP residue Glu^{73} is an anti-canonical residue. As previously noted, glutamate 73 forms hydrogen bonds with the backbone amino groups of Tyr^{105} and Ser^{106} of TEM-1 (8). The E73A mutant shows a small decrease in isoenthalpic temperature, suggesting a slight increase in hydrophilic interactions. This is unexpected since the mutant loses the side chain responsible for hydrophilic interactions. One explanation is the loss of the negatively charged side chain of Glu^{73} may allow a better electrostatic interaction between BLIP $Lys^{74}$and TEM-1 and/or elimination of van der Waals repulsion between the sidechain of Glu^{73} and the backbone of the TEM-1.

Among the hotspot contact residues, two residues, Lys^{74} and Trp^{150}, demonstrate anti-canonical behavior. Mutant K74A displays a decrease in isoenthalpic temperature, suggesting the loss of the charged side chain actually results in a loss of hydrophobic interactions rather than hydrophilic interactions. This suggests that the side chain of Lys^{74} may be involved in intramolecular interactions that increase the entropy driving forces for TEM-1 binding. Inspection of the structure of the complex indicates the Lys^{74} nitrogen interacts with the oxygen of the backbone carbonyl between Gly^{141} and Phe^{142} (Figure 7). This intramolecular interaction appears to be holding the second loop (aa 136-144) like a flap onto itself and the TEM-1 surface. This loop has three residues that contact TEM-1- Phe^{142}, Tyr^{143} and Arg^{144}. A recent report shows that this loop can undergo large rearrangements depending upon the binding target (36). This suggests that Lys74 plays a role in the flexibility and energetic coupling with loop 2. Finally, the W150A mutant exhibits an increase in the isoenthalpic temperature suggesting the loss of the hydrophobic portion of the residue actually results in a loss of hydrophilic interactions. Future structural elucidation of this complex may reveal the detailed mechanism of this interaction.

Based on this analysis, we hypothesize that the interactions between the canonical hotspot contact residues and the TEM-1 β-lactamase target protein are energetically favorable interactions that provide direct contributions to the binding free energy. The anti-canonical contact residues may interact with TEM-1 through a combination of energetic coupling with other contact residues and possible structural modifications. The interpretation of these results is based largely on consideration of BLIP alone. We assume TEM-1 β-lactamase changes little between binding wild type BLIP versus a mutant BLIP. However, we cannot rule out that the observed thermodynamics are due to changes of both BLIP and TEM-1 in the complex in response to the BLIP mutation. Ultimately, these possibilities must be examined by elucidating the structures of the complexes of TEM-1 β-lactamase and the BLIP mutants and such studies are in progress.

Finally, the information generated here will be useful as a guide for future mutagenesis efforts to develop BLIP derivatives with altered binding properties. For example, it will be of interest to determine if mutations in BLIP that alter its binding specificity occur preferentially at residues in the canonical or anti-canonical categories.

Acknowledgements
The authors wish to thank Dr. Gillian Lynch for technical assistance. This work was support in part by a Scientist Development Grant from American Heart Association (0435186N) and startup funding from University of Houston and the Institute for Molecular Design (to D.C.) and National Institutes of Health Grant AI32956 (to T.P.)

REFERENCES

1. Nooren, I. M., and Thornton, J. M. (2003) *Embo J* **22**, 3486-3492
2. Janin, J. (1995) *Proteins* **21**, 30-39
3. Lo Conte, L., Chothia, C., and Janin, J. (1999) *J Mol Biol* **285**, 2177-2198
4. Nooren, I. M., and Thornton, J. M. (2003) *J Mol Biol* **325**, 991-1018
5. Brooijmans, N., Sharp, K. A., and Kuntz, I. D. (2002) *Proteins* **48**, 645-653
6. Wells, J. A. (1990) *Biochemistry* 29, 8509-8517
7. Schreiber, G., and Fersht, A. R. (1995) *J Mol Biol* **248**, 478-486
8. Zhang, Z., and Palzkill, T. (2003) *J Biol Chem* **278**, 45706-45712
9. Clackson, T., and Wells, J. A. (1995) *Science* **267**, 383-386
10. Bogan, A. A., and Thorn, K. S. (1998) *J Mol Biol* **280**, 1-9
11. Chothia, C., and Janin, J. (1975) *Nature* **256**, 705-708
12. Ackers, G. K., and Smith, F. R. (1985) *Annu Rev Biochem* **54**, 597-629
13. Sundberg, E. J., and Mariuzza, R. A. (2002) *Adv Protein Chem* **61**, 119-160
14. Calderone, C. T., and Williams, D. H. (2001) *J Am Chem Soc* **123**, 6262-6267
15. Stites, W. E. (1997) *Chem Rev* **97**, 1233-1250
16. Bush, K., Jacoby, G. A., and Medeiros, A. A. (1995) *Antimicrob Agents Chemother* **39**, 1211-1233
17. Majiduddin, F. K., Materon, I. C., and Palzkill, T. G. (2002) *Int J Med Microbiol* **292**, 127-137
18. Doran, J. L., Leskiw, B. K., Aippersbach, S., and Jensen, S. E. (1990) *J Bacteriol* **172**, 4909-4918
19. Strynadka, N. C., Jensen, S. E., Alzari, P. M., and James, M. N. (1996) *Nat Struct Biol* **3**, 290-297
20. Zhang, Z., and Palzkill, T. (2004) *J Biol Chem* **279**, 42860-42866
21. Rudgers, G. W., and Palzkill, T. (2001) *Protein Eng* **14**, 487-492
22. Rudgers, G. W., Huang, W., and Palzkill, T. (2001) *Antimicrob Agents Chemother* **45**, 3279-3286
23. Janin, J. (1995) *Biochimie* **77**, 497-505
24. Veselovsky, A. V., Ivanov, Y. D., Ivanov, A. S., Archakov, A. I., Lewi, P., and Janssen, P. (2002) *J Mol Recognit* **15**, 405-422
25. Sigurskjold, B. W. (2000) *Anal Biochem* **277**, 260-266
26. Zhang, Y. L., and Zhang, Z. Y. (1998) *Anal Biochem* **261**, 139-148
27. Emsley, P., and Cowtan, K. (2004) *Acta Crystallogr D Biol Crystallogr* **60**, 2126-2132
28. (1994) *Acta Crystallogr D Biol Crystallogr* **50**, 760-763
29. Black, S. D., and Mould, D. R. (1991) *Anal Biochem* **193**, 72-82
30. Petrosino, J., Rudgers, G., Gilbert, H., and Palzkill, T. (1999) *J Biol Chem* **274**, 2394-2400
31. Strynadka, N. C., Jensen, S. E., Johns, K., Blanchard, H., Page, M., Matagne, A., Frere, J. M., and James, M. N. (1994) *Nature* **368**, 657-660
32. Wiseman, T., Williston, S., Brandts, J. F., and Lin, L. N. (1989) *Anal Biochem* **179**, 131-137
33. Velazquez-Campoy, A., Leavitt, S. A., and Freire, E. (2004) *Methods Mol Biol* **261**, 35-54
34. Turnbull, W. B., and Daranas, A. H. (2003) *J Am Chem Soc* **125**, 14859-14866
35. Selzer, T., Albeck, S., and Schreiber, G. (2000) *Nat Struct Biol* **7**, 537-541
36. Reynolds, K. A., Thomson, J. M., Corbett, K. D., Bethel, C. R., Berger, J. M., Kirsch, J. F., Bonomo, R. A., and Handel, T. M. (2006) *J Biol Chem* **281**, 26745-26753

FIGURE LEGENDS

Figure 1. Isothermal titration calorimetric measurements of the binding of TEM-1 β-lactamase and BLIP. Raw isothermal titration calorimetric curves of the interaction of TEM-1 β-lactamase and BLIP at two different temperatures (A). At 10 °C (left panel), the binding has a positive enthalpy of + 5.1 kcal mol^{-1}. At 30 °C (right panel), the binding has a negative enthalpy of –7.4 kcal mol^{-1}. However, the transition regions of the curves are sharp and narrow, giving erroneous K values. (B) Plot of binding enthalpies vs temperatures and the slope of the linear regression yields a binding heat capacity change of –667 cal mol^{-1} K^{-1}.

Figure 2. Isothermal titration calorimetric measurements of the binding of TEM-1 β-lactamase and BLIP mutants. Raw isothermal titration calorimetric curves of the interaction of TEM-1 β-lactamase and low affinity BLIP mutant W150A at 6 °C (A) and of TEM-1 and low affinity BLIP mutant K74A at 25 °C (B). The transition regions of the curves are relatively smooth yielding accurate K values in addition of the enthalpies. Detail numerical results are listed in the Table 1.

Figure 3. Comparison of changes of binding thermodynamics for the binding of BLIP alanine mutants to TEM-1 β-lactamase at 15 °C. The solid bars represent the difference in binding free energy (ΔG_{mut} $-\Delta G_{wt}$). The hatch bars represent the difference in binding enthalpy (ΔH_{mut} $-\Delta H_{wt}$). The open bars represent the difference in binding entropy terms ($T\Delta S_{mut}$ $-T\Delta S_{wt}$). The binding free energy is calculated from the average of several measurements. The binding enthalpy at 15°C is calculated using the isoenthalpic temperatures (T_H) and the binding heat capacity changes (ΔCp) from Table 1. The binding entropy terms are calculated using $-T\Delta S=\Delta G-\Delta H$. The positive values indicate the loss of driving forces. For clarity, no error bar is presented.

Figure 4. Plot of changes of hydrophobicity due to alanine substitution of a positions versus the changes of isoenthalpic temperatures. The changes of hydrophobicity are the difference between the hydrophobicity scale of the wild type amino acid and that of alanine. The hydrophobicity scale is used according to Black & Mould (1991). The squares represent residues that exhibit properties that are canonical and the triangles represent residues with anti-canonical properties (see discussion section for definition).

Figure 5. Graphical representation of the TEM-1 β-lactamase binding thermodynamics results for the contact residues of BLIP. The non-contact portion of BLIP is represented as a molecular surface. The contact residues are represented as either VDW for hotspot residues or bonds for nonhotspot residues. Red indicates canonical and green indicates anti-canonical residues as defined in the text. The Tyr50 contact residue is labeled with a bold arrow to indicate that its alanine mutant increases affinity. Several contact residues are not labeled including Ser^{39}, Gly^{48}, Ser^{71} and Ser^{113}.

Figure 6. Structural representation of the interactions between TEM-1 β-lactamase and residues His^{41}, Asp^{49}, and Tyr^{50}. The Tyr^{50} residue, shown as bonds, is located between Asp^{49} and His^{41} which are shown as VDW. TEM-1 is represented as an orange molecular surface. Despite the indentation on TEM-1 to accommodate the Tyr^{50} side chain, the removal of the side chain will allow even better interactions between Asp^{49} and His^{41} with TEM-1.

Figure 7. Structural representation of interactions between loop 2 of BLIP with BLIP residue Lys^{74} and with TEM-1 β-lactamase. Three residues, Gly^{141}, Phe^{142}, and Tyr^{143} of BLIP loop 2 and Lys^{74} are displayed as a CPK representation and TEM-1 is depicted as an orange molecular surface. Note the closeness (2.94 Å) between the nitrogen (blue) of the Lys^{74} side chain and the oxygen (red) of the carbonyl of the loop 2 backbone. This proximity could be important for guiding Phe^{142} and loop 2 into the cleft of TEM-1.

Table 1. Thermodynamic parameters for wild-type BLIP and alanine substitution mutants of BLIP contact residues.

Mutant	Ki [nM]	K [$10^8 M^{-1}$]	N	ΔH [kcal/mol]	ΔS [cal/(mol K)]	T_{exp} [°C]	ΔG [kcal/mol]	ΔCp [cal/(mol K)]	T_H[°C]
Low affinity mutants									
F36A	40 ± 15	0.14 ± 0.02	0.89 ± 0.01	-10.2 ± 0.2	-1.0 ± 0.7	30	-9.9 ± 0.1	-653 ± 25	16.3 ± 0.6
		0.21 ± 0.01	0.98 ± 0.01	-4.1 ± 0.1	19.9 ± 0.1	25	-9.4 ± 0.1		
		0.53 ± 0.06	1.09 ± 0.01	6.4 ± 0.1	58.2 ± 0.4	6	-9.9 ± 0.1		
H41A	34 ± 10	0.26 ± 0.01	1.10 ± 0.01	-5.1 ± 0.2	17.1 ± 0.5	28	-10.2 ± 0.1	-592 ± 12	19.4 ± 0.4
		0.19 ± 0.01	1.11 ± 0.01	6.5 ± 0.2	56.3 ± 0.6	8	-9.4 ± 0.1		
		0.08 ± 0.01	1.14 ± 0.01	8.1 ± 0.2	61.0 ± 0.8	6	-8.9 ± 0.1		
D49A	20 ± 4	0.38 ± 0.03	1.15 ± 0.01	6.0 ± 0.1	55.6 ± 0.3	15	-10.0 ± 0.1	-271 ± 21	37.7 ± 2.9
		0.51 ± 0.02	1.13 ± 0.01	7.8 ± 0.1	63.0 ± 0.3	10	-10.0 ± 0.1		
		0.67 ± 0.04	1.10 ± 0.01	8.4 ± 0.1	66.0 ± 0.4	6	-10.0 ± 0.1		
Y53A	21 ± 2	0.40 ± 0.04	0.99 ± 0.01	-7.2 ± 0.1	11.0 ± 0.4	30	-10.6 ± 0.1	-544 ± 8	16.8 ± 0.2
		0.14 ± 0.01	0.92 ± 0.01	5.1 ± 0.1	50.8 ± 0.3	8	-9.2 ± 0.1		
		0.29 ± 0.01	1.05 ± 0.01	5.6 ± 0.1	54.1 ± 0.3	6	-9.5 ± 0.1		
K74A	46 ± 8	0.11 ± 0.01	1.07 ± 0.01	-8.7 ± 0.1	3.6 ± 0.3	30	-9.8 ± 0.1	-510 ± 5	12.8 ± 0.1
		0.09 ± 0.01	0.95 ± 0.01	-6.3 ± 0.1	10.6 ± 0.3	25	-9.5 ± 0.1		
		0.16 ± 0.01	1.05 ± 0.01	3.5 ± 0.1	45.3 ± 0.2	6	-9.2 ± 0.1		
W112A	13 ± 3	0.28 ± 0.03	1.03 ± 0.01	-8.8 ± 0.2	4.9 ± 0.7	30	-10.3 ± 0.1	-518 ± 12	12.1 ± 0.3
		0.40 ± 0.03	1.12 ± 0.01	-8.5 ± 0.2	6.6 ± 0.7	28	-10.5 ± 0.1		
		0.64 ± 0.02	1.14 ± 0.01	3.3 ± 0.1	47.5 ± 0.4	6	-10.0 ± 0.1		
F142A	16 ± 3	0.38 ± 0.04	1.10 ± 0.01	-6.5 ± 0.1	13.3 ± 0.4	30	-10.5 ± 0.1	-521 ± 6	17.8 ± 0.2
		0.26 ± 0.02	1.09 ± 0.01	5.3 ± 0.1	52.9 ± 0.3	8	-9.5 ± 0.1		
		0.38 ± 0.03	1.02 ± 0.01	6.0 ± 0.1	56.3 ± 0.4	6	-9.7 ± 0.1		
H148A	21 ± 2	1.44 ± 0.08	0.67 ± 0.01	-8.2 ± 0.2	10.3 ± 0.7	30	-11.3 ± 0.1	-667 ± 25	18.4 ± 0.7
		0.20 ± 0.04	0.82 ± 0.01	5.6 ± 0.2	53.0 ± 0.9	12	-9.5 ± 0.1		
		0.13 ± 0.02	0.83 ± 0.01	7.4 ± 0.3	59.0 ± 1.3	6	-9.1 ± 0.1		
W150A	184 ± 52	0.02 ± 0.001	1.13 ± 0.01	7.5 ± 0.1	54.9 ± 0.3	15	-8.4 ± 0.1	-275 ± 28	32.4 ± 3.3
		0.04 ± 0.002	0.90 ± 0.01	8.5 ± 0.2	60.3 ± 0.4	10	-8.6 ± 0.1		
		0.02 ± 0.001	1.02 ± 0.01	10 ± 0.2	64.6 ± 0.4	6	-8.1 ± 0.1		
R160A	11 ± 2	0.21 ± 0.01	1.05 ± 0.01	6.3 ± 0.1	55.3 ± 0.3	15	-9.7 ± 0.1	-458 ± 26	28.6 ± 1.6
		0.37 ± 0.04	1.15 ± 0.01	9.1 ± 0.1	66.9 ± 0.5	8	-9.7 ± 0.1		
		0.34 ± 0.03	1.04 ± 0.01	10.6 ± 0.2	72.3 ± 0.5	6	-9.6 ± 0.1		
High affinity mutants									
S39A	0.3 ± 0.1	N/D	1.13 ± 0.01	2.7 ± 0.1		20	-13.0 (*)	-606 ± 51	23.9 ± 2.0
		N/D	1.07 ± 0.01	4.9 ± 0.1		15			
		N/D	1.00 ± 0.01	9.9 ± 0.2		8			
		N/D	1.03 ± 0.01	10.9 ± 0.2		6			
G48A	0.7 ± 0.2	N/D	0.96 ± 0.01	-4.7 ± 0.1		30	-12.5(*)	-575 ± 25	21.8 ± 0.9
		N/D	1.11 ± 0.01	8.2 ± 0.2		8			
		3.4 ± 1.0[a]	1.15 ± 0.01	8.9 ± 0.2		6	-11 ± 0.5		
Y50A	0.011 ± 0.004	3000 ± 300[b]	1.09 ± 0.01	-10.2 ± 0.1		30	-16 ± 0.5	-417 ± 17	5.6 ± 0.2
		N/D	1.15 ± 0.01	-7.9 ± 0.1		25			
		3225 ± 320[b]	1.12 ± 0.01	-3.9 ± 0.1		15	-15 ± 0.5		
Y51A	0.5 ± 0.03	13.1 ± 1.3[c]	1.11 ± 0.01	-9.5 ± 0.1		30	-12.6 ± 0.5	-809 ± 37	18.9 ± 0.9
		15.0 ± 1.5[c]	1.04 ± 0.01	-4.4 ± 0.1		25	-12.5 ± 0.5		
		N/D	1.06 ± 0.01	7.6 ± 0.1		10			
		15.6 ± 1.6[c]	1.06 ± 0.01	10.0 ± 0.1		6	-11.7 ± 0.5		
S71A	0.2 ± 0.06	N/D	0.97 ± 0.01	-3.2 ± 0.1		30	-13.2(*)	-488 ± 53	23.6 ± 2.6
		N/D	1.02 ± 0.01	6.1 ± 0.1		12			
		N/D	0.98 ± 0.01	8.3 ± 0.2		6			
E73A	0.4 ± 0.06	N/D	0.80 ± 0.01	-9.1 ± 0.6		30	-12.8(*)	-651 ± 18	16.0 ± 0.4
		N/D	0.84 ± 0.01	-7.7 ± 0.2		28			
		N/D	0.85 ± 0.01	-6.6 ± 0.2		26			
		N/D	1.00 ± 0.01	6.5 ± 0.2		6			
S113A	0.11 ± 0.006	N/D	1.02 ± 0.01	2.5 ± 0.1		15	-13.6(*)	-769 ± 183	18.8 ± 4.5
		N/D	1.00 ± 0.01	7.6 ± 0.2		10			
		N/D	0.97 ± 0.01	9.4 ± 0.2		6			
G141A	1.8 ± 0.2	N/D	0.99 ± 0.01	-11.9 ± 0.2		30	-11.9(*)	-797 ± 44	15.1 ± 0.8
		N/D	1.07 ± 0.01	6.1 ± 0.2		8			
		N/D	0.97 ± 0.01	6.8 ± 0.2		6			
Y143A	0.6 ± 0.2	20 ± 2[a]	1.15 ± 0.01	3.8 ± 0.1		25	-12.7 ± 0.3	-641 ± 89	30.8 ± 3.9
		N/D	1.15 ± 0.01	10.2 ± 0.1		15			
		N/D	1.14 ± 0.01	11.6 ± 0.1		12			
		N/D	1.15 ± 0.01	14.2 ± 0.1		8			
		6.5 ± 0.6[a]	1.11 ± 0.01	15.6 ± 0.7		6	-11.3 ± 0.2		
R144A	0.6 ± 0.2	N/D	0.87 ± 0.01	-6.6 ± 0.2		30	-12.6(*)	-506 ± 38	18.2 ± 1.4
		N/D	0.95 ± 0.01	-4.3 ± 0.1		28			
		N/D	0.88 ± 0.01	4.9 ± 0.1		8			
		N/D	0.89 ± 0.01	6.4 ± 0.2		6			
WT	0.5 ± 0.1	90 ± 10[d]	1.03 ± 0.01	-7.4 ± 0.1		30	-13.8 ± 0.5	-667 ± 51	18.8 ± 0.9
		N/D	1.07 ± 0.01	-4.1 ± 0.1		25			
		N/D	1.09 ± 0.01	5.1 ± 0.1		10			
		N/D	1.05 ± 0.01	9.2 ± 0.1		6			

K_is are the previously reported inhibition concentration (8).
K values were determined by standard ITC for low affinity BLIP mutants.

(a) This K value was determined using displacement ITC with F142A as the displaced low affinity mutant.
(b) This K value was determined using displacement ITC with W150A as the displaced low affinity mutant.
(c) This K value was determined using displacement ITC with R160A as the displaced low affinity mutant.
(d) This K value was determined using displacement ITC with Y51A as the displaced affinity mutant.
N/D indicates nondetermined values due to lack of successful displacement ITC measurements.
For high affinity BLIP mutants, no entropy is calculated because of the potential errors of the K values.
* these free energies are calculated from published K_is for 25 °C.

Figure 1

A

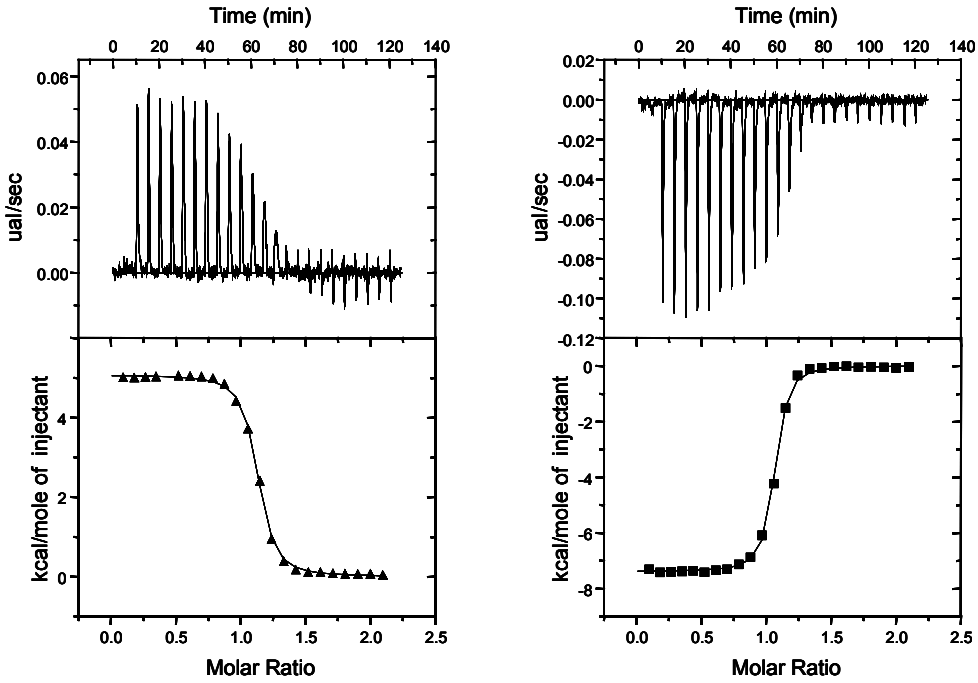

B

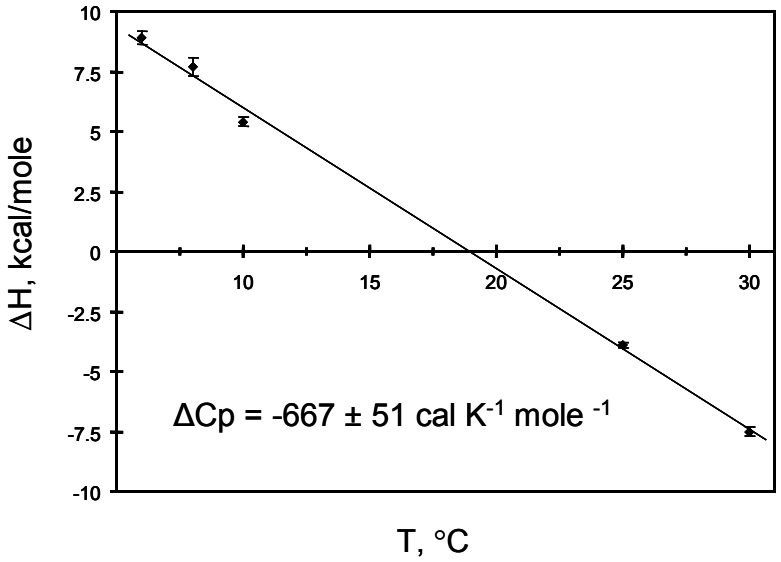

Figure 2

A

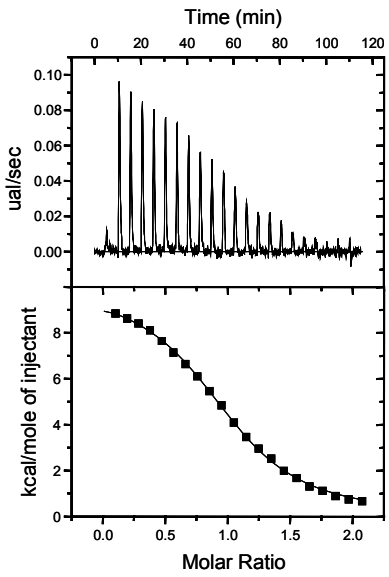

W150A at 6 °C

B

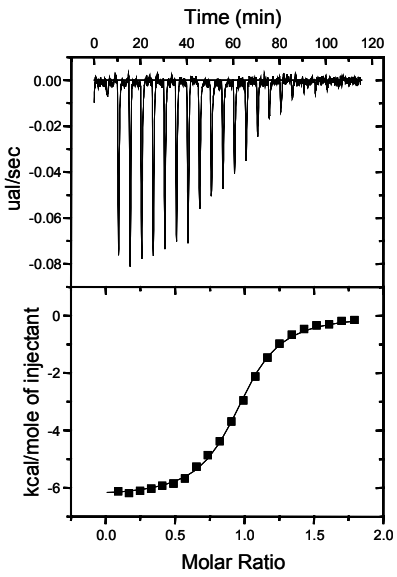

K74A at 25 °C

Figure 3

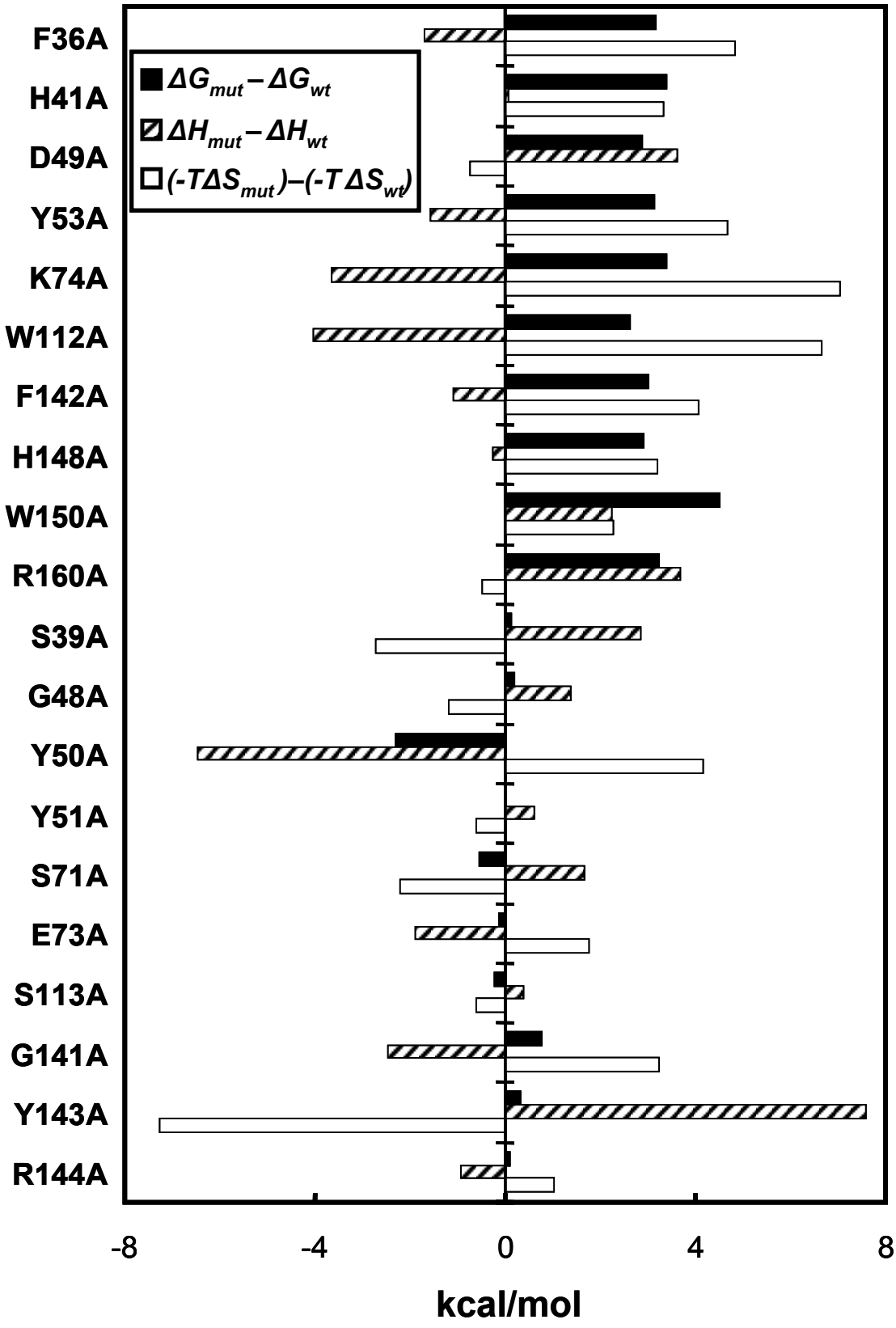

Figure 4

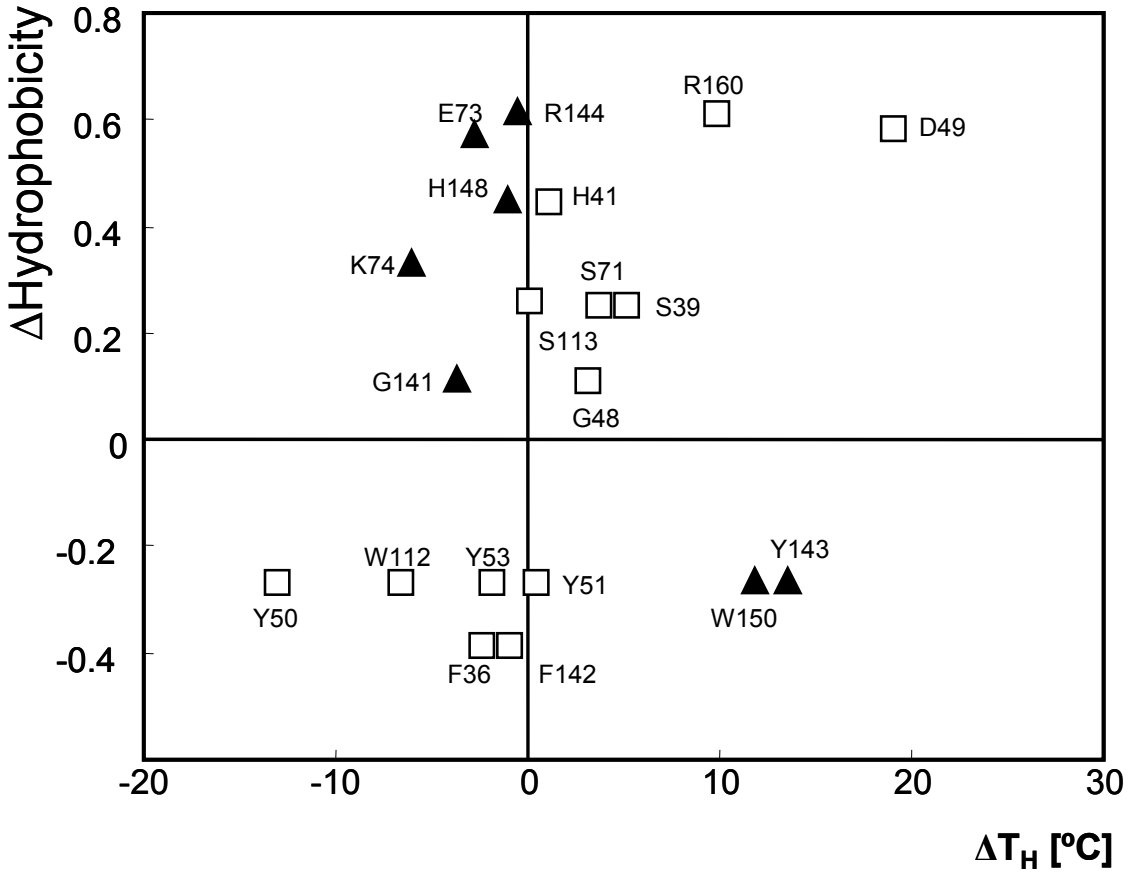

Figure 5

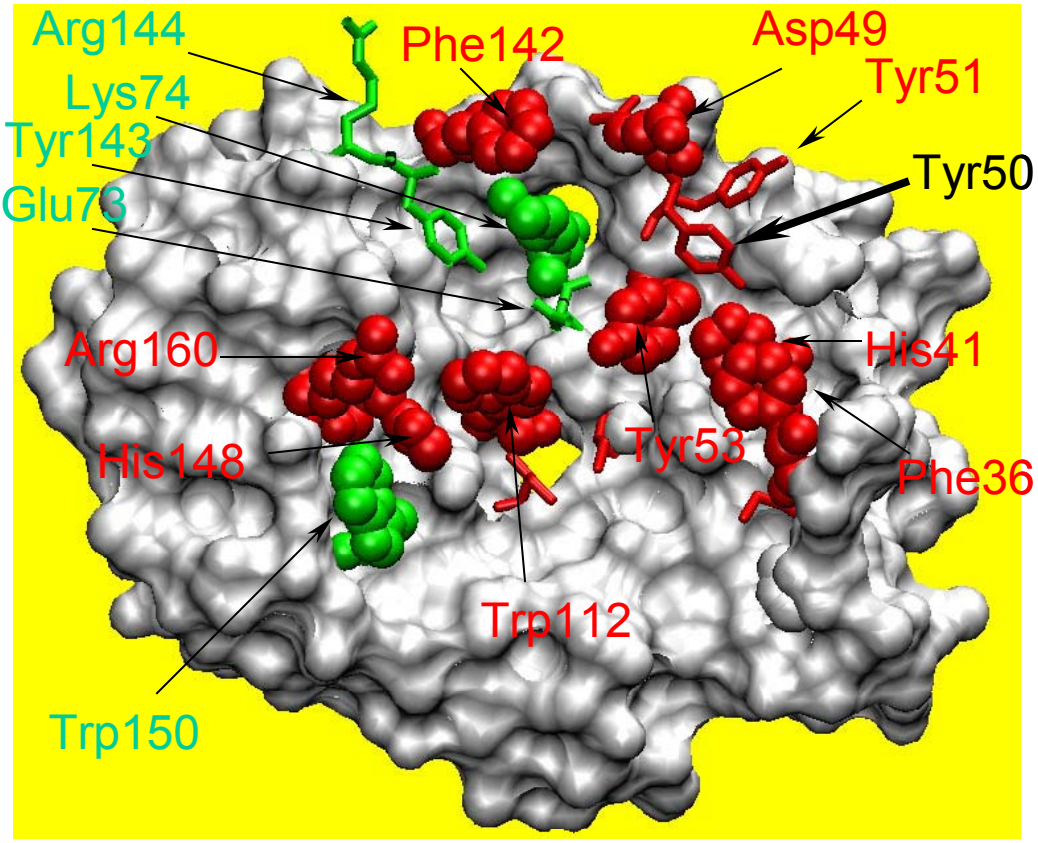

Figure 6

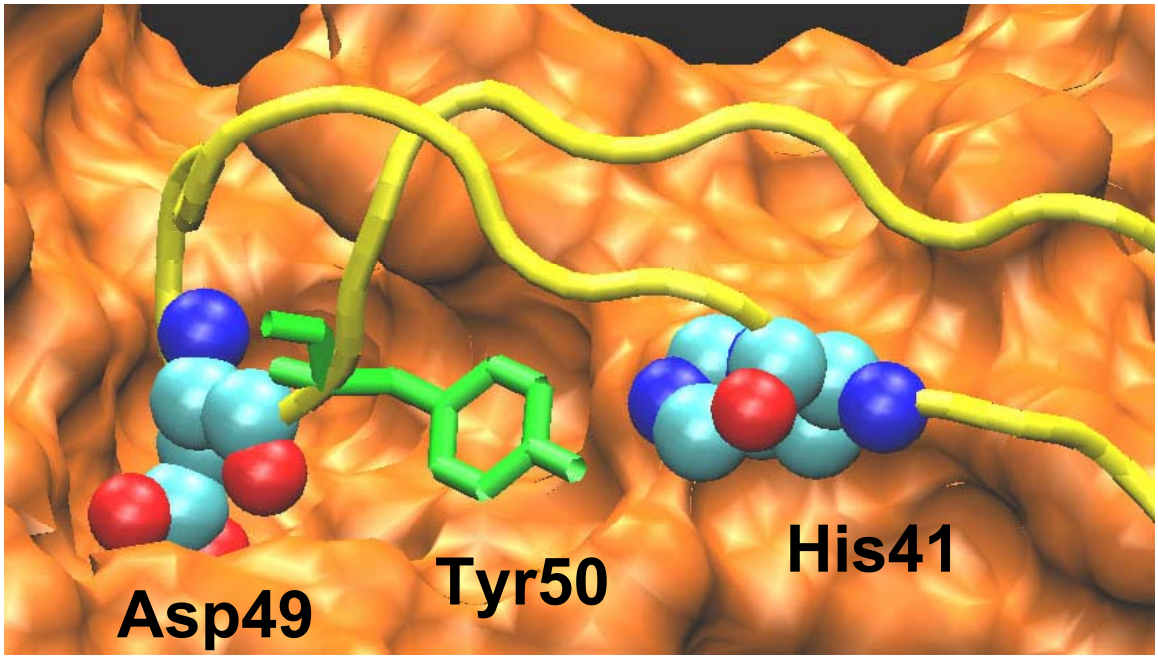

Figure 7

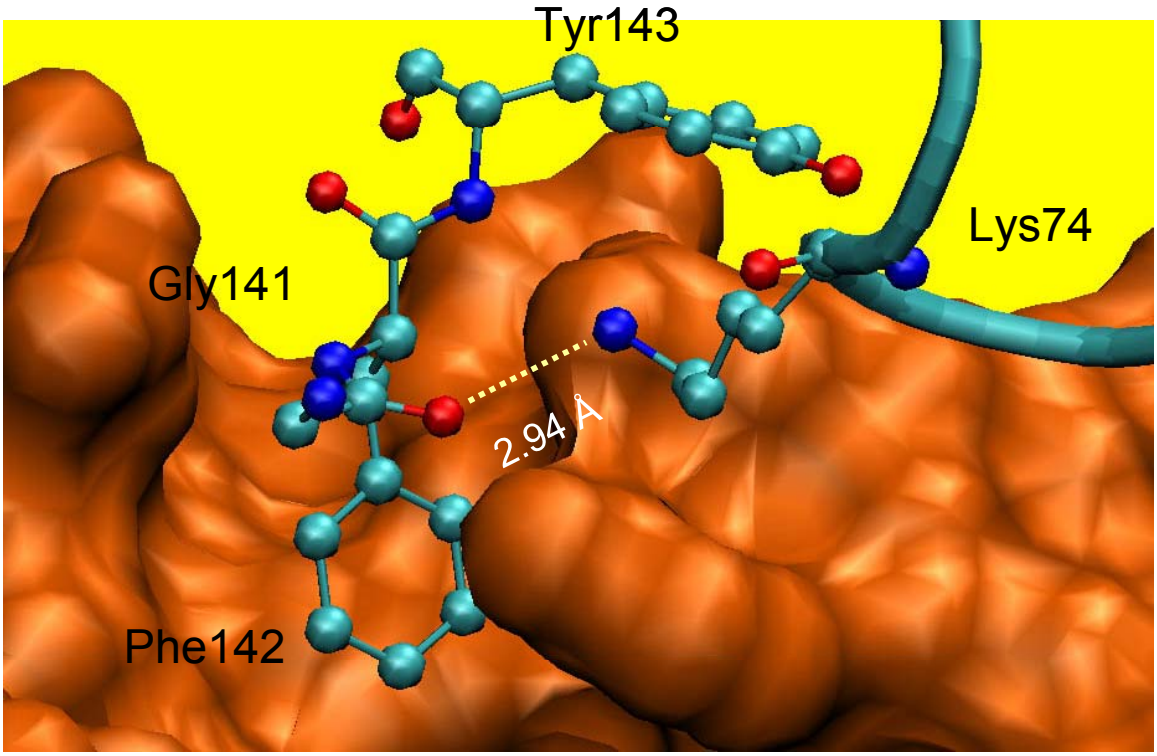

Thermodynamic investigation of the role of contact residues of blip for binding to tem-1 β-lactamase

Jihong Wang, Zhen Zhang, Timothy Palzkill and Dar-Chone Chow

J. Biol. Chem. published online April 12, 2007
